Proceedings of The National Conference
On Undergraduate Research (NCUR) 2014
University of Kentucky, Lexington, KY
April 3-5, 2014

Contribution of the N-terminal Domain of Human Lysyl-tRNA Synthetase to tRNALys Binding

Jacob Calhoun
Department of Chemistry
University of Cincinnati
Cincinnati, Ohio 45219 USA

Faculty Advisor: Dr. Pearl Tsang

Abstract

In addition to the canonical function of charging tRNALys with lysine, Lysyl-tRNA synthetase (LysRS) associates with the HIV-1 proteins Gag and Gag-Pol in a process that enables selective incorporation of tRNALys3 into budding HIV-1 virions, where tRNALys3 primes reverse transcription upon infection by HIV. Mutant LysRS studies have shown tRNALys is incorporated significantly less in LysRS mutants lacking the N-terminal domain, demonstrating the N-terminal domain's contribution to tRNALys binding as well as apparent cooperative binding of the synthetase's domains. The goal of this research is to quantitate the affinity of the N-terminal domain for tRNALys variants. This is accomplished by cloning, over-expression and purification of recombinant forms of the N-terminal domain of human LysRS in E. coli (BL21 DE3). Following the isolation of the N-terminal domain of LysRS, we proceeded to quantify the N-terminal domain's affinity for tRNALys3 and derivatives, using techniques such as EMSA. Since it was previously demonstrated by comparative NMR studies that this N-terminal domain is primarily unstructured in the absence of RNA, the results of these binding studies will be interpreted based upon the protein's structure in order to better understand how this domain influences RNA binding by LysRS.

Keywords: LysRS, N-terminal domain (NTD), tRNA, EMSA, HIV-1

1. Introduction

Lysyl-tRNA Synthetase (LysRS) is an enzyme that catalyzes the ligation, or "charging," of a tRNA molecule with the amino acid lysine for protein production. In bacteria, it consists of two domains; one for binding the anticodon of the tRNA for proper recognition, and a catalytic domain at the C-terminus of the protein. In higher eukaryotes however, there is an additional N-terminal domain (NTD) whose function is not well understood (Figure 1). It's been shown that this domain greatly increases HIV-1's selective incorporation of tRNALys3, the only one of three isoacceptors able to prime reverse transcription of the HIV-1 genome[1, 2, 3, 4]. Because of this evidence, we set out to quantify binding of the NTD to RNA oligonucleotides mimicking portions of the full tRNALys. This was done by first expressing recombinant forms of the NTD in Escherichia coli (BL21 DE3 cell line).

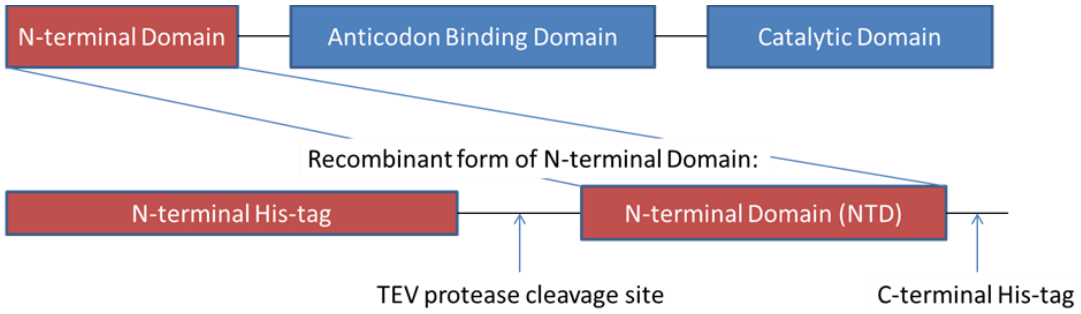

Figure 1. Schematic of LysRS Protein: At the top, the domain structure of full human form of LysRS including the NTD. At the bottom, the recombinant form of just the NTD is shown. The form of NTD studied, called RMN, has both an N-terminal and C-terminal His-tag. A more recent form that we used lacks the C-terminal tag and is called MNT. Both forms contain a TEV cleavage site for removing the N-terminal His-tag.

2. Methods

The method to produce a pure sample of the NTD protein consisted of first transforming cells with a plasmid vector coding for NTD with the lactose promoter for easy induction by IPTG, and an antibiotic (Kanamycin) resistance gene so non-transformed cells could not be used for large culture growths. To be sure the cell colonies selected would produce NTD in a large volume culture, an induction test was done on small volume cultures (usually 5mL). NTD expression was visualized on SDS-PAGE gels (Figure 2). Colonies showing highest increase of NTD production were used to inoculate larger volumes of media (0.5L) which were incubated and subsequently induced at a standard optical density (OD) of 0.3-0.6 (at 600nm). The OD600 is a good indicator for cell density. This induction was also checked by SDS-PAGE. The cultures were then spun down, rinsed with phosphate buffered saline (PBS) to remove remaining media and froze at -20 degrees centigrade until NTD purification.

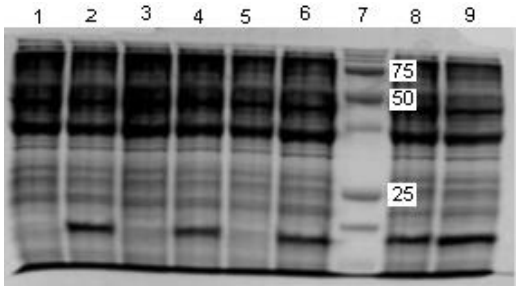

Figure 2. Protein Induction SDS-PAGE: From left to right the samples correspond to pre-induction culture A, then post-induction (with IPTG), next pre- and post-induction for culture B, and pre- and post-induction for culture C. The molecular weight marker following C post-induction shows the NTD fusion protein runs between the 15 and 20kDa bands.

Purification of the NTD from the frozen cell pellet was done by resuspending the cells in a lysis solution containing protease inhibitors and detergents to break open the cell membrane. Alternatively, a French Press was used to break the cells using high pressure. The lysate was then subjected to centrifugation for various times (20 minutes to 1hr) to separate the soluble and insoluble fractions. Since LysRS is a cytoplasmic enzyme, the NTD is in the soluble portion. This was then placed onto a Nickel-sepharose resin column (GE Amersham) which is used for binding Histidine residues (therefore affinity chromatography). While the recombinant NTD binds, the remaining cell debris passes through. NTD is then removed from the column by increasing concentrations of imidazole, a chemical structurally similar to histidine and competes for binding the resin. This procedure is also checked by SDS-PAGE (Figure 3).

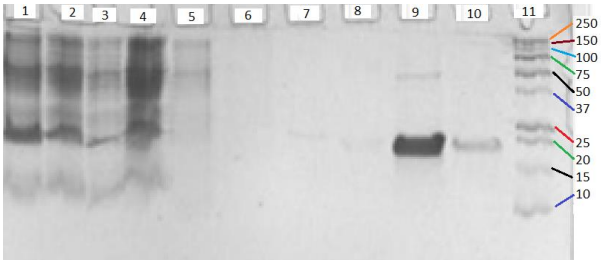

Figure 3. Nickel Column purification monitored by SDS-PAGE: Lanes 1-3 are samples before addition to the column followed by the load (lane 4) containing cellular proteins that did not bind. Buffer is washed over the resin (lanes 6-8) to remove nonspecifically bound species before removing NTD with imidazole in lanes 9 and 10. The masses of the protein molecular weight markers are shown in lane 11. .

Once the NTD was isolated and dialyzed into the appropriate TEV buffer, TEV protease was added to the dialysis bag. This reaction was often done overnight at room temperature to reach complete cleavage. As before, the reaction results were checked by SDS-PAGE (Figure 4). The sample now containing TEV protease and two fragments of the NTD were subjected to ion-exchange chromatography, using a positively charged diethylaminoethyl (DEAE) resin. This is efficacious because each species has a different isoelectric point (pI) and so in buffers at pH 7.5, the larger fragment (target NTD peptide) is positively charged and so passes through the resin while the smaller His-tag peptide binds (being negatively charged at this pH). This was also tested by SDS-PAGE visualization (Figure 5). Finally, the isolated NTD is purified of RNAse contamination by Nickel chromatography in which the short C-terminal his tag of the NTD binds to the resin and RNAse washes off. RNAse contamination was tested following this procedure by an RNAse Alert assay. The kit provides synthetic RNA as a substrate that also contains a fluorescent molecule that is seen by UV light if the RNA substrate is digested by RNAse (Figure 6). RNAse must be kept to a minimum to effectively measure binding in assays using RNA.

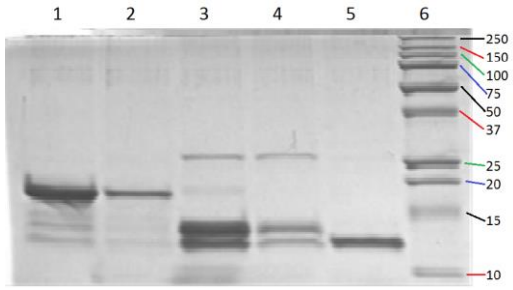

Figure 4. TEV Protease Cleavage SDS-PAGE: Lanes 1 and 2 are samples containing fusion NTD before TEV addition. Lanes 3 and 4 show samples taken at 14hr after addition. Fusion protein is completely gone in lane 4 demonstrating complete cleavage. The new higher band near the 25kDa marker band is TEV protease. A His-tag standard is shown in the lane just before the marker and matches the lower band in the cleaved samples.

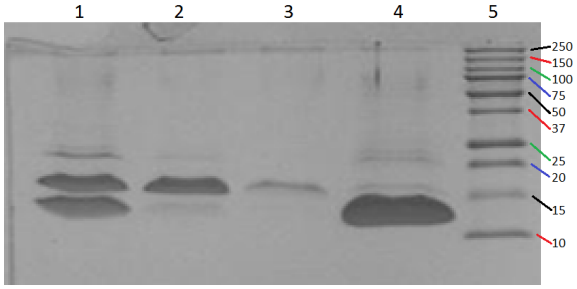

Figure 5. DEAE Column SDS-PAGE: The pre-column sample containing TEV protease, and both NTD fragments are shown in Lane 1. The load is in lane 2, followed by a buffer wash (lane 3); both contain the upper NTD fragment

only. Lane 4 corresponds to the lower (His-tag) fragment and TEV protease that bound to the DEAE and were removed by increasing NaCl concentrations. Lane 5 corresponds to the molecular weight markers with their masses to the right of the gel.

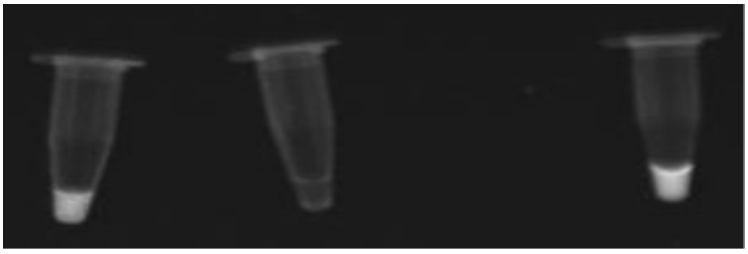

Figure 6. RNase Alert Assay Following Affinity Chromatography: To test for the presence of RNase, a test substrate was incubated with the protein sample being assayed. If RNase is present, the substrate fluoresces as a result of RNase activity. The negative control (Nickel equilibration buffer only, middle) shows no fluorescence and therefore no RNase activity. The tube on the right shows activity in the pre nickel treatment as does the tube on the left (post Ni treatment). Taking into account overall sample fluorescence as well as total protein concentrations, the post-Nickel sample has approximately half the RNase contamination.

2.1 Protein Quantitation

Quantitating the NTD required different methods depending on the recombinant form being isolated and purified. These methods include bichonchinic acid (BCA) assays, UV (280) measurements, and spot densitometry. Ideally, UV is best because it is the most rapid, and a spectra of wavelengths can be visualized to identify contaminants. This requires amino acids with chromophoric side chains, of which RMN has none after cleavage by TEV protease. For working with RMN after this stage, spot densitometry was used most often for several reasons. The main reason is that BCA assays are not tolerant of imidazole. Often, RMN is passed through a Nickel affinity column to remove any rnase after it is separated from the His-tag. This step puts RMN in a buffer with imidazole, which would require an extra dialysis step to perform a BCA with. This extra step is susceptible to protein loss and takes several hours. Spot densitometry is not buffer-dependent and so this extra step is not required.

Spot densitometry was conducted using pictures of SDS-PAGE gels that were run using the protein sample (RMN) along with a standard protein of known concentration. The idea is that a given amount of a specific peptide will absorb the same amount of stain in any gel. This does not mean that the integrated density values (IDVs) will not vary from gel to gel, but that the relative IDVs between the sample and standard will not change. Different peptides can also be used for standards. RMN standards were more difficult to obtain than commercial proteins like Bovine Serum Ablumin (BSA). All that was done in order to use BSA as a standard was to standardize a range of BSA amounts against previous RMN standards, preventing the continued use of RMN standards for spot densitometry. The best way to utilize spot densitometry is to use two standard concentrations in which the sample is in the range of. This is because IDVs are not linear and they begin to level off at higher concentrations. It was found that if the RMN sample was in the range of BSA loaded on a gel, there would be about 1.5x as much RMN than was estimated by a curve generated from BSA standard IDVs (table 1). For MNT, this was very close to the actual amount. When samples began to exceed the range of BSA, this factor of underestimation increased. When samples were in the range of one order of magnitude, the factor varied between 2 and 3. When this was exceeded, the factors became sporadic, varying between 32 and 80. Accurate estimates of protein require some idea of concentration so the correct range of BSA can be selected or so the sample can be diluted to within the range of BSA.

Table 1 Bovine Serum Ablumin (BSA) and standard Integrated Density Values (IDVs)

pg93	ug	IDV	curve	factor
RMNfp	2.7	22438	1.801888	1.498428
BSA	0.4	12656		
BSA	1	17985		
BSA	2	27180		
BSA	4	32999		
pg149	ug	IDV	curve	factor
BSA	0.1	4743		
BSA	0.4	13137		
BSA	1	16929		
RMNdb	8.4	52634	3.780102	2.222162
RMNdb	16.8	44690	3.14504	5.341745
MNT70	4.26	35348	2.398217	1.776319
MNT70	2.13	27890	1.802007	1.182016
MNT70	1.07	19772	1.153034	0.927987
MNT50	3.05	31861	2.119458	1.439047
MNT50	1.52	25241	1.590239	0.955831
MNT50	0.76	14847	0.759317	1.000899

Spot densitometry of NTD: The first column corresponds to the peptide gel band. The next column shows the amount of protein loaded in each gel well in micrograms. The middle column is the IDV value assigned by the software (AlphaEase FC) autocorrecting for background. The column titled "curve" is the amount of protein (ug) estimated from the curve generated by that gel's BSA standards. The last column is the factor of underestimation. This value was obtained by dividing the actual amount of NTD by that estimated by the curve. RMNfp refers to fusion protein, RMNdb refers to the "double-banded" form of RMN (see Degradation section), and MNT70 and 50 refer to MNT standards of 70 and 50uM, respectively.

3. Results

3.1 RNA Binding Assays

The primary method to determine binding values for RMN was electrophoretic mobility shift assays (EMSAs). The basic concept is that a constant amount of RNA is used in each sample with increasing amounts of protein. Samples are submitted to electrophoresis in a polyacrylamide gel and stained to visualize where the RNA migrates. Free RNA is small and moves fastest. As protein is increased, more of the total RNA binds. The bound complex is larger and therefore moves slower through the gel. EMSAs were done in our lab[10] using the anticodon stem-loop oligomer with either RMN, full length LysRS, or 2 domain (2D) protein which consists of just the anticodon binding domain and the catalytic domain of LysRS. EMSAs are in Figure 7a-c. The graphs in figure 8 show the percentage of RNA bound versus the concentration of protein with the final Kd values listed in table 2.

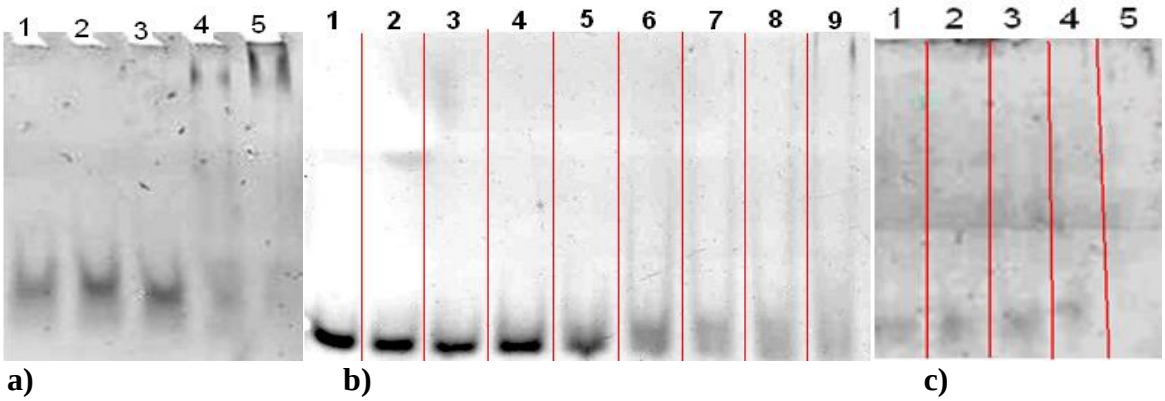

Figure 7. EMSA Results of NTD Binding: Figure 7a (left) shows an EMSA of the anticodon stem-loop (ACSL) with full length LysRS. Starting with 0uM protein in the first lane, protein concentration increases until ACSL starts visibly binding (loss of lower free band intensity) at 0.46uM in the fourth lane. Figure 7b (middle) shows the ACSL with 2D protein. Here, binding starts at 0.53uM. Figure 7c (right, with red lines added to clarify lanes) shows an EMSA of the ACSL with RMN and full length LysRS. The first lane is free RNA, followed by two samples with RMN (lanes 2 and 3), and then full length in lanes 4 and 5 as a control. Binding was not observed with RMN even at concentrations greater than three times the estimated Kd value. Concentrations of ACSL were 160nM.

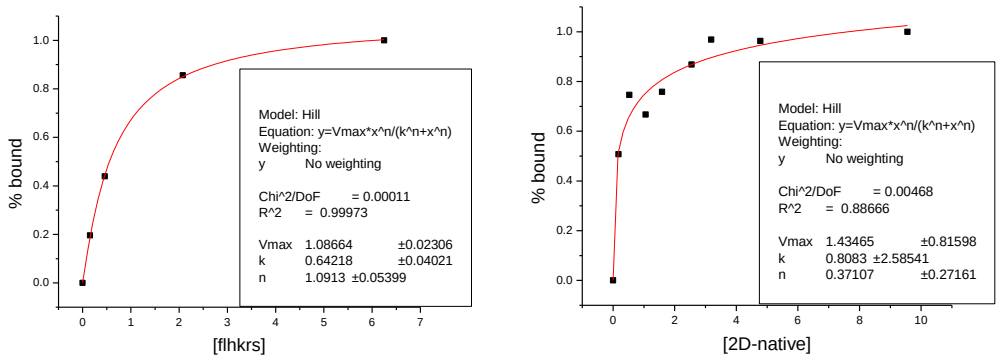

Figure 8. EMSA Plots: The plot on the left corresponds to the EMSA in figure 7a, while the plot on the right corresponds to the EMSA in 7b. As protein concentrations increase (x-axis), more RNA becomes bound and the percent is shown on the y-axis. The box in each shows the results of fitting the data with the Hill equation.

Table 2. Peptide and Kd Values

Peptide	Kd (uM)
FLHKRS	0.642
2D	0.808

Binding constants by EMSA: The two peptides used in EMSA experiments are listed in the left column while the Kd values are listed in the right in uM. The Kd value is the concentration of protein at which 50% of the substrate (in this case, ACSL) is bound.

From the EMSAs, Kd values were calculated via spot densitometry for full length LysRS and 2D that were 0.642uM and 0.808uM (table 2), respectively. This similarity in Kd values suggests very little contribution of binding to the anticodon stem-loop by RMN, and direct binding of RMN to ACSL is not detectable by EMSA at the concentrations used.

A complementary binding method used was fluorescence anisotropy (FA) and the binding of RMN to different RNA oligonucleotides were carried out by our collaborators at The Ohio State University (8, K. Musier-Forsyth, unpublished data). This method measures variances in the intensities of polarized light. Basically, the degree of change in polarization depends on the size of the molecule and its movements ("tumbling") in solution. When the fluorophore (RNA) is bound to protein, the complex tumbles less than free RNA in solution. This difference describes the affinity of the protein and RNA. They tested four different RNA oligonucleotides - native tRNALys3, an oligonucleotide mimicking the anticodon stem-loop, one mimicking the acceptor stem-loop, and one mimicking the tRNA-like element (TLE) of the HIV-1 genome with four cytosines in the loop ("TLE-4C"). The general trend of RMN binding affinities determined this way was in general agreement with our EMSA results (data not shown).

3.2 Degradation of NTD

Under some conditions, such as RNAse removal before cleavage by TEV or longer periods between steps, an elusive extra band can be observed (Figure 8).

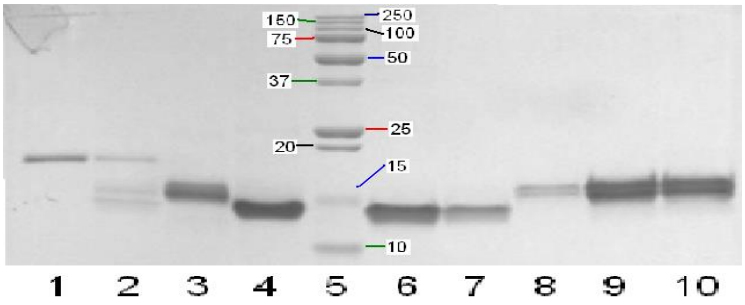

Figure 8. Double Bands of Upper NTD Fragment by SDS-PAGE: SDS-PAGE following TEV cleavage. Lanes 1-4 show the pre cleavage fusion NTD, a 21hr TEV cleavage sample, an NTD standard, and then a His-tag standard, respectively. After the marker (lane 5, with molecular weight labels in kDa) are two His-tag standard samples (lanes 6 and 7) followed by other NTD samples (lanes 8, 9, and 10) that have two upper bands, neither of which correlate to the His-tag fragment or the fusion NTD.

Careful observation of Figure 7 will show that the last three samples contain two bands of similar mobility as the larger cleaved NTD fragment. Neither band seems to correlate to any known peptide in the procedure. For this reason, we suspected degradation to be the case.

Our lab has previously witnessed deamidation of protein samples, as evidenced by mass spectrometry (Liu 2012, 7). The deamidation is thought to occur at asparagine residues followed by a number of possible residues, most notably glycine (Geiger 1987, 6). The proposed mechanism involves nucleophilic attack of the side chain amide group of Asn by the backbone Nitrogen of the following amino acid, forming a cyclic succinimide intermediate (Figure 8).

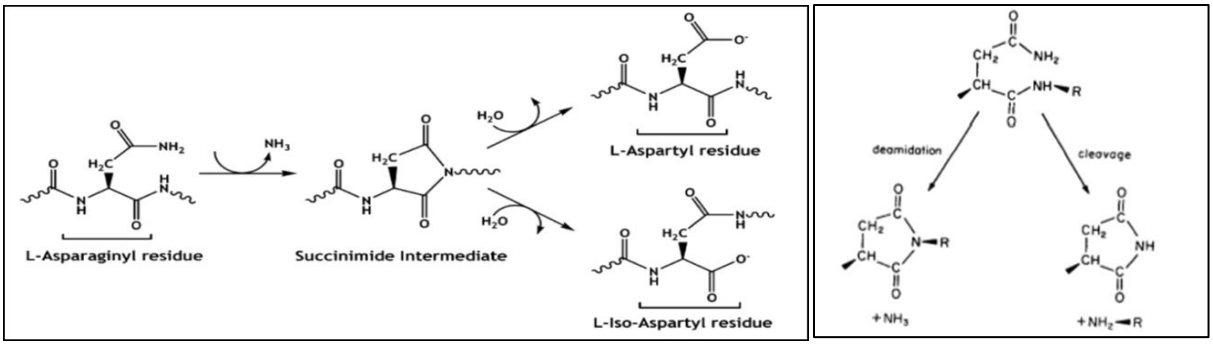

Figure 9. Mechanisms of Degradation: The reaction in the box above shows the replacement of the Asn residue by either an Asp residue or an iso-Aspartyl residue while keeping the peptide intact[5]. The bottom shows two possible fates following attack by the backbone Nitrogen. It may deamidate, or result in cleavage of the peptide[6].

One study tested various synthetic hexapeptides containing an asparagine residue followed by a glycine, proline, or leucine residue[6]. They observed only deamidation and isomerization in those followed by glycine, but cleavage products were seen when Asn was followed by Pro or Leu. While the recombinant NTD does contain an Asn-Leu sequence, we don't expect this to be a point of cleavage, since it is within the TEV site and the degradation appears to happen after cleavage. Because degradative cleavage proceeds through the same intermediate as deamidation, it is possible that it may still occur at an Asn-Gly sequence (which is present in the larger cleaved NTD fragment). Some supporting evidence is previous NMR work in our lab on the NTD in the absence of RNA showing that the NTD is relatively unstructured (7). This lack of structural restriction would make degradation more likely due to increased intramolecular interactions. To find out, we requested a mass spec of the sample (8) to identify the molecular weight of the bands (Figure 9).

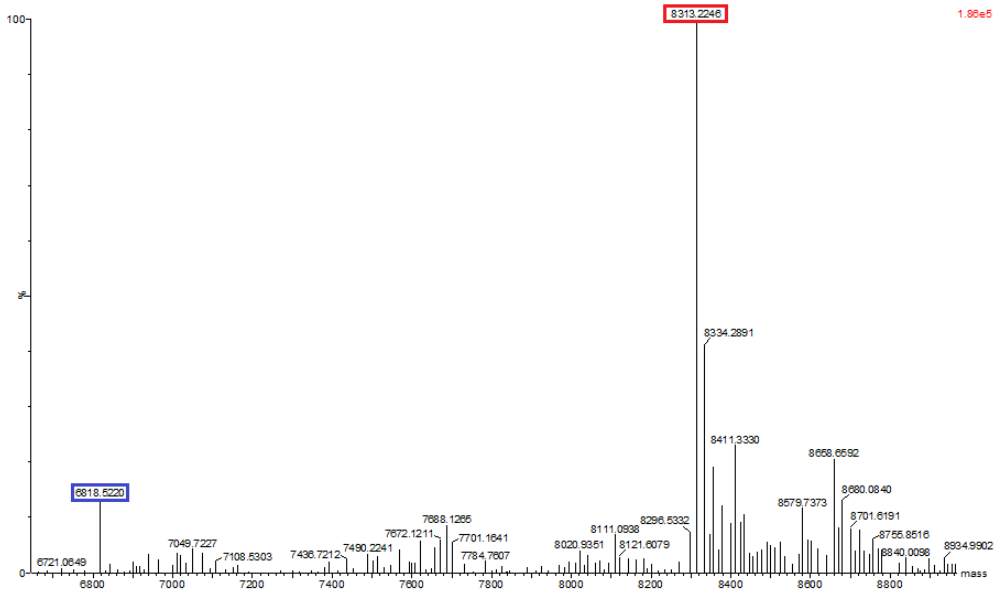

Figure 9. Electrospray Ionization Mass Spectrometry of NTD Double Bands: The large signal (boxed in red) corresponds to 8313.2 Da mass is due to the TEV-cleaved NTD which should be 8311.3. With a difference of 2Da, this is within error of the equipment. The largest peak to the left of this gives a mass of 6818.5 Da (boxed in blue). This undoubtedly corresponds to the lower degraded band in the SDS-PAGE gels.

The mass spec results are inconclusive in terms of directly supporting deamidation, since the mass increase of 1 Da would not be discernable from error for peptides above 8000 Da. The smaller mass given was unexpected.

Considering cleavage at the Asn-Gly sequence, we calculate a mass of 6777 Da. There is a mass reading of 6778Da, which is likely this cleavage product with a proton. The most notable peak below 8313 was 6818Da, 41Da higher than expected.

4. Conclusions and Future Work

Without RNA, RMN has little defined structure and the resulting flexibility of the protein is likely to increase its susceptibility to deamidation and degradation since bond angle rotations are less restricted[7]. The nature of the prominent mass measurement of 6818Da in the mass spec data is still unknown. Further work may include tandem mass spec to determine the sequence of amino acids and compare it to the non-degraded sequence. If this Asn-Gly sequence is the cause of nonenzymatic cleavage, then we can substitute Asn with other amino acids to reduce degradation rates and improve purification yields. Literature also suggests higher pH and temperatures increase rates of deamidation and so should be better avoided (such as the pre-TEV DEAE treatment to remove RNAse at pH 8.5) as well as reducing time between purification steps.

FA experiments show that RMN binds more strongly to the acceptor stem-loop than the ACSL (data not shown), although EMSAs do not indicate that it binds to the ACSL. RMN also demonstrated highest binding to full length tRNA by FA (data not shown). One possibility to describe this observation is that RMN binds to the ACSL and acceptor stem-loop at different parts of the peptide and could be binding to two full length tRNA molecules simultaneously. Another more likely explanation for the higher binding affinity to the full-length tRNA is that it could contain a separate binding site not mimicked in any of the oligomers tested that is more optimal for binding RMN. One could test this idea by synthesizing RNA oligonucleotides mimicking other structural portions of the tRNA such as the D loop or TψC loop and test their binding properties to RMN for comparison. Other work would include EMSAs using the acceptor stem-loop oligonucleotide since binding of RMN is indicated by FA to be higher and more likely to be detected than with the ACSL. More binding studies can be done with base substitutions in RNA oligonucleotides to provide clues about the binding requirements of RMN and determining whether any bases specifically bind RMN.

Although degradation seems like an undesirable effect of the isolation procedure, literature suggests several functional roles of deamidation in the cell[6]. Deamidation can be reversed by an enzyme or can signal a protein for degradation by the proteasome. Dubbed a potential "molecular clock," Asn residues may provide regulatory roles in protein metabolism and therefore environmental response. LysRS (in eukaryotes) is involved in other cell functions such as the immune response, and serving as part of a Multi-synthetase complex (MSC). Deamidation can also very likely alter a protein's structure and function. Future work can explore implications of LysRS deamidation on HIV-1 pathology and other cellular processes.

5. Acknowledgements

The author wishes to express his appreciation to Dr. Stephen Macha for mass spectroscopy, Roopa Coomandur and Dr. Karin Musier-Forsyth for FA experiments, Sruthi Sundaram of our group for performing the EMSAs, Dr. Sheng Liu for previous NMR work on RMN and full length LysRS, Dr. Pearl Tsang for mentorship, and The University of Cincinnati for use of facilities.

6. References

1) Cen, Shan, Hassan Javanbakht, Meijuan Niu, and Lawrence Kleiman. "Ability of Wild-Type and Mutant Lysyl-tRNA Synthetase to Facilitate tRNALys Incorporation into Human Immunodeficiency Virus Type 1." Journal of Virology 78.3 (2004): 1595-601.

2) Kovaleski, Brandie J., Robert Kennedy, Minh K. Hong, Siddhartha A. Datta, Lawrence Kleiman, Alan Rein, and Karen Musier-Forsyth. "In Vitro Characterization of the Interaction between HIV-1 Gag and Human Lysyl-tRNA Synthetase." The Journal of Biological Chemistry 281.28 (2006): 19449-9456.

3) Francin, M., Kaminska, M. and Mirande, M. "The N-terminal domain of mammalian Lysyl-tRNA synthetase is a functional tRNA-binding domain". J. Biol Chem. (2002) 277(3), 1762-9.

4) Kleiman, Lawrence, Christopher P. Jones, and Karin Musier-Forsyth. "Formation of the $tRNA^{Lys}$ packaging complex in HIV-1." FEBS letters 584.2 (2010): 359-365.
5) Catak, Saron, et al. "Reaction mechanism of deamidation of asparaginyl residues in peptides: effect of solvent molecules." The Journal of Physical Chemistry A 110.27 (2006): 8354-8365.
6) Geiger, Terrence, and S. Clarke. "Deamidation, isomerization, and racemization at asparaginyl and aspartyl residues in peptides. Succinimide-linked reactions that contribute to protein degradation." Journal of Biological Chemistry 262.2 (1987): 785-794.
7) Liu, S., Ph.D. thesis, University of Cincinnati, 2012.
8) Musier-Forsyth, K. and Coomandur, Roopa, fluorescence anisotropy, The Ohio State University, 2014. Unpublished data.